Regenerative Therapy 4 (2016) 92–102

Contents lists available at ScienceDirect

Regenerative Therapy

journal homepage: http://www.elsevier.com/locate/reth

Original article

Cardiac fibroblast-derived VCAM-1 enhances cardiomyocyte proliferation for fabrication of bioengineered cardiac tissue

Takahiro Iwamiya [a, 1], Katsuhisa Matsuura [b], Shinako Masuda [a], Tatsuya Shimizu [a], Teruo Okano [a, *]

[a] Institute of Advanced Biomedical Engineering and Science, Tokyo Women's Medical University, Japan
[b] Institute of Advanced Biomedical Engineering and Science, Department of Cardiology, Tokyo Women's Medical University, Japan

ARTICLE INFO

Article history:
Received 31 October 2015
Received in revised form
15 January 2016
Accepted 18 January 2016

Keywords:
Cell sheets
ES cell
Cardiomyocyte
Fibroblasts
VCAM-1

ABSTRACT

Background: Fibroblasts are indispensable for the fabrication of cell-sheet–based bioengineered cardiac tissues; however, whether cardiac fibroblasts can improve tissue properties for transplantation or *in vitro* models compared with other fibroblast types remains unclear. We compared the cell organization and functional properties of cardiomyocyte sheets derived from co-culture with different fibroblast types and investigated the molecular mechanisms for the observed differences.

Methods and results: Cardiac cell sheets were fabricated by co-culturing mouse embryonic stem cell (ESC)-derived cardiomyocytes with mouse neonatal cardiac fibroblasts (NCFs), mouse adult cardiac fibroblasts (ACFs), and mouse adult dermal fibroblasts (ADFs). Cardiac cell sheets obtained from NCF or ACF co-culture showed numerous uniformly distributed and functional (beating) cardiomyocytes, while cell sheets obtained by co-culture with ADFs showed fewer and aggregated cardiomyocytes. The greater number of cardiomyocytes in the presence of NCFs was because of enhanced cardiomyocyte proliferation, as revealed by protein markers of mitosis and BrdU incorporation. Microarray analysis revealed that NCFs expressed substantially higher levels of vascular cell adhesion molecule-1 (VCAM-1) than ADFs. Treatment of ESC-derived cardiomyocytes in monoculture with soluble VCAM-1 significantly increased the number of functional cardiomyocytes, while the enhancement of cardiomyocyte number by co-culture with NCFs was abolished by anti-VCAM-1 antibodies.

Conclusions: Cardiac fibroblasts enhance the proliferation of ESC-derived cardiomyocytes through VCAM-1 signaling, leading to an increase in functional myocardial cells in bioengineered tissue sheets. These sheets may be advantageous for cell-based therapy and *in vitro* heart research.

1. Introduction

Fibroblasts exist in almost all vertebrates, where they form and stabilize the three-dimensional structure of tissues by secreting extracellular matrix components. Fibroblasts respond to tissue injury and ischemia by proliferating and depositing new extracellular matrix to aid in repair [1]. However, severe injury may result in excessive fibroblast proliferation, resulting in fibrosis and concomitant loss of tissue function. Myocardial infarction and cardiomyopathies can result in cardiomyocyte loss, creating voids that are filled by fibrous tissue; this fibrosis can lead to cardiac remodeling and heart failure [2]. Cardiac fibroblasts secrete neurohumoral factors such as angiotensin II and endothelin-1 which are known to contribute to cardiac remodeling via blood pressure elevation, cardiomyocyte apoptosis, and local inflammation [3].

During development, cardiac fibroblasts form a network of cell processes and collagen fibers to guide myocyte organization. Fibroblasts promote embryonic cardiomyocyte proliferation, an indispensable process for forming thick ventricular walls, through β1 integrin signaling [4]. However, the identity of the cardiac fibroblast-derived promitotic factor remains unclear. Moreover, cell-cell interactions between cardiac fibroblasts and embryonic

* Corresponding author. 8-1 Kawada-Cho, Shinjuku-Ku, Tokyo 162-8666, Japan. Tel.: +81 3 5367 9945; fax: +81 3 3359 6046.
E-mail address: tokano@twmu.ac.jp (T. Okano).
Peer review under responsibility of the Japanese Society for Regenerative Medicine.
[1] Present address: Institute for Advanced Biosciences, Keio University.

http://dx.doi.org/10.1016/j.reth.2016.01.005

cardiomyocytes critical for cardiac development, repair, and pathogenesis have not been elucidated in detail.

Mechanisms of myocyte–fibroblast signaling are important not only for understanding heart development and pathogenesis but also for heart tissue engineering. We are developing a cell-sheet–based cardiac tissue engineering method using temperature-responsive culture dishes. Layering cardiac cell sheets containing neonatal rat-derived cardiomyocytes, fibroblasts, and endothelial cells on vascular beds enables the fabrication of viable, vascularized cardiac tissue [5–7]. This cell-sheet–based tissue engineering does not require a scaffold but requires an extracellular matrix. Thus, the presence of fibroblasts is indispensable for fabrication of cardiac cell sheets from purified embryonic stem cell (ESC)-derived cardiomyocytes [8]. Recent reports have suggested that cell–cell interactions between cardiomyocytes and non-myocytes, such as cardiac fibroblasts, are important for heart physiology and repair [9]. Thus, use of cardiac fibroblasts may improve the fabrication of cardiac tissue for transplantation and *in vitro* studies. However, whether cardiac fibroblasts have a specific development function or are interchangeable with fibroblasts from other tissues for cardiomyocyte proliferation and function remains unclear.

Here we demonstrate that cardiac fibroblasts, but not dermal fibroblasts, promote the proliferation of mouse ESC-derived cardiomyocytes and facilitate the development of functional cardiac cell sheets. Cardiac fibroblasts expressed higher levels of VCAM-1 than dermal fibroblasts. We show that release of VCAM-1 from cardiac fibroblasts facilitates cardiac myocyte proliferation and distribution of functional (contracting) cardiomyocytes in bio-engineered cardiac tissue sheets.

2. Methods

2.1. Animals and reagents

This study was carried out in strict accordance with the recommendations in the Guide for the Care and Use of Laboratory Animals of Tokyo Women's Medical University. All experimental protocols were approved by the Institutional animal care and use committee of Tokyo Women's Medical University. All efforts were made to minimize suffering. Wild-type C57BL/6 mice were purchased from Japan SLC (Shizuoka, Japan) and B6 Cg-Tg (CAG-DsRed*MST) 1Nagy/J mice from The Jackson Laboratory (Bar Harbor, ME).

The following antibodies were used for immunocytochemistry, enzyme-linked Immunosorbent assay (ELISA), and flow cytometry: rabbit polyclonal anti-discoidin domain receptor tyrosine kinase 2 (DDR2) (GeneTex, Irvine, CA), guinea pig monoclonal anti-vimentin (Progen, Heidelberg, Germany), mouse monoclonal anti-NG2 (Millipore, Temecula, CA), rabbit polyclonal anti-alpha smooth muscle actin (αSMA) (Abcam, Cambridge, UK), mouse monoclonal anti-cardiac troponin T (cTnT) (Thermo Scientific, Rockford, IL), mouse monoclonal anti-cytokeratin11 (EXBIO, Nad Safinou, CZ), rabbit polyclonal anti-Ki67 (Abcam), rabbit polyclonal anti-phospho-histone H3 (phospho S10) (Abcam), rat monoclonal anti-integrin α4β1 (Abcam), and recombinant mouse VCAM-1/CD106 Fc chimera (R&D Systems, Minneapolis, MN). Secondary antibodies against guinea pig, mouse, rabbit, and rat were purchased from Jackson ImmunoResearch Laboratories (West Grove, PA). Unless otherwise specified, all reagents were purchased from Sigma–Aldrich (St. Louis, MI).

2.2. Mouse embryonic stem cell cultures

The methods for isolation and maintenance of mouse ESC (mESC)-derived cardiomyocytes expressing yellow fluorescent protein (YFP) and the neomycin phosphotransferase gene under control of the α-myosin heavy chain promoter were described previously [8]. In that study, we reported that more than 99% of cells were positive for myosin heavy chain, about 98% for sarcomeric α-actinin, and about 85% for cardiac troponin T (cTnT).

2.3. Fibroblast isolation

Fibroblasts were obtained from 1 day old (neonatal) and 10–12 weeks old (adult) wild-type C57BL/6 mice as described previously [8]. Neonatal cardiac fibroblasts (NCFs) were used for experiments after the third passage. Adult cardiac fibroblasts (ACFs) and adult dermal fibroblasts (ADFs) were obtained using the explant culture method. For isolation of NCFs and ACFs, fresh mouse hearts (P1 or 10–12 weeks of age, respectively) were washed with phosphate buffered saline (PBS) and cut into approximately 4 mm^2 pieces. These pieces were covered with sterilized cover glasses and cultured in DMEM supplemented with 10% FBS on 10 cm diameter culture dishes. Two weeks after seeding, cells were dissociated with 0.25% trypsin/EDTA and sub-cultured to other 10 cm dishes. ACFs from passage 3 were used for experiments. Adult dermal fibroblasts (ADFs) were obtained from dorsal dermal tissue of adult mice (10–12 weeks of age). Harvested dermal tissues were treated with dispase I (1000 U/mL) (Eidea, Ibaraki, Japan) overnight at 4 °C and then cut into approximately 25 mm^2 pieces. These pieces were covered with sterilized cover glasses and cultured in DMEM supplemented with 10% FBS on 10 cm culture dishes. Two weeks after seeding, cells were dissociated with 0.25% trypsin/EDTA and sub-cultured on 10 cm dishes. ADFs from passage 3 were used for the experiments.

In some experiments, NCFs and ADFs were isolated from CAG-DsRed*MST 1Nagy/J mice (Neonatal: 1 day, Adult: 10 weeks) using the same methods.

2.4. Cell sheet preparation

Before seeding cells, temperature-responsive culture dishes (UpCell; CellSeed, Tokyo, Japan) were incubated with fetal bovine serum (FBS) for 2 h mESC-derived cardiomyocytes were co-cultured with each type of fibroblasts at a ratio of 8:2 with DMEM supplemented with 10% FBS (Fibroblasts = 5.4×10^4 cells/cm^2; cardiomyocytes = 2.16×10^5 cells/cm^2). After 5 days, co-cultures were incubated at 20 °C to detach the cell sheets. Bright field images of co-cultures were obtained using a Nikon ECLIPSE Ti microscope (Nikon, Tokyo, Japan).

2.5. Electrophysiological analysis

Extracellular field potentials from cardiomyocyte sheets were measured by a multi-electrode array (MED) system (Alpha MED Sciences, Osaka, Japan) as described previously [8].

2.6. Immunocytochemistry

Cells were fixed with 4% paraformaldehyde and immunostained as described [8]. Immunostaining was analyzed using an ImageXpress Ultra Confocal High Content Screening System and MetaExpress software (Molecular Devices, CA).

2.7. Flow cytometry analysis of BrdU incorporation

Cells (5×10^5 per trial) were incubated in cell culture medium containing 10 μM BrdU. BrdU staining and analysis were performed according to an instruction manual (BD Pharmingen, Franklin Lakes, NJ). Cells were fixed and permeabilized with BD

Cytofix/Cytoperm Buffer, then exposed to BrdU in solution with DNase. BrdU staining was performed with APC-anti-BrdU antibody (BD Pharmingen, Franklin Lakes, NJ). Samples were analyzed with a Gallios fluorescence activated cell sorting (FACS) system (Beckman Coulter, Brea, CA). The following reagents were used for analysis: BD Cytofix/Cytoperm Buffer, BD Perm/Wash Buffer (10×), BD Cytoperm Plus Buffer (10×), BrdU, and DNase (all from BD Pharmingen).

2.8. Time-lapse photography

Images were acquired over five days using a BZ-9000 fluorescence microscope maintained in humidified air containing 5% CO_2 at 37 °C (Keyence, Osaka, Japan).

2.9. RNA extraction and microarray analysis

From fibroblasts (NCFs and ADFs), total RNA was extracted using TRIzol reagent (Invitrogen, Carlsbad, CA) according to the manufacturer's instructions and further purified using the Qiagen RNeasy Mini Kit (QIAGEN, Valencia, CA) according to the manufacturer's instructions. RNA quantity and quality were determined using a Nanodrop ND-1000 spectrophotometer (Thermo Fisher Scientific Inc., Waltham, MA) and an Agilent Bioanalyzer (Agilent Technologies) as recommended.

For cRNA amplification and labeling, total RNA was amplified and labeled with cyanine 3 (Cy3) using Agilent Low Input Quick Amp Labeling Kit, one-color (Agilent Technologies) following the manufacturer's instructions. Briefly, 100 ng of total RNA was reverse transcribed to double-stranded cDNA using a poly dT-T7 promoter primer. Primer, template RNA, and quality-control transcripts of known concentration and quality were first denatured at 65 °C for 10 min and then incubated for 2 h at 40 °C with 5 × first strand Buffer, 0.1 M DTT, 10 mM dNTP mix, and AffinityScript RNase Block Mix. The AffinityScript enzyme was inactivated by heating to 70 °C for 15 min cDNA products were then used as templates for *in vitro* transcription to generate fluorescent cRNAs. cDNA products were mixed with a transcription master mix in the presence of T7 RNA polymerase and Cy3-labeled CTP and incubated at 40 °C for 2 h. Labeled cRNAs were purified using QIAGEN's RNeasy mini spin columns and eluted in 30 μL of nuclease-free water. After amplification and labeling, cRNA quantity and cyanine incorporation were determined using a Nanodrop ND-1000 spectrophotometer and an Agilent Bioanalyzer. For sample hybridization, 1.65 μg of Cy3-labeled cRNA was fragmented and hybridized to an Agilent Mouse GE 4 × 44 K v2 Microarray (Design ID: 026655) at 65 °C for 17 h. After washing, microarrays were scanned using an Agilent DNA microarray scanner.

For analysis of microarrays, intensity values of each scanned feature were quantified using Agilent feature extraction software version 10.7.3.1, which performs background subtraction. We only used features that were flagged as “no errors” (present flags) and excluded features that were not positive, not significant, not uniform, not above background, saturated, or were population outliers (marginal and absent flags). Normalization was performed using Agilent GeneSpring GX version 11.0.2. (per chip: normalization to 75 percentile shift; per gene: normalization to median of all samples). There are 39,429 probes on the Agilent Mouse GE 4 × 44 K v2 Microarray (Design ID: 026655) excluding control probes.

The altered transcripts were quantified using the comparative method. We applied a ≥2-fold change in signal intensity as the threshold to identify significant differences in gene expression between NCFs and ADFs.

2.10. Quantitative real-time PCR analysis

Complementary DNA was generated from total RNA using the High Capacity cDNA Reverse Transcription Kit (Applied Biosystems, Foster City, CA), PCR-related primers, and TaqMan Universal PCR Master Mix (Applied Biosystems). Each RT-PCR reaction was run for 10 min at 25 °C, 120 min at 37 °C, and 5 s at 85 °C using an iCycler (BIO-RAD). A 1-μg sample of cDNA was used from each run. TaqMan probe real-time PCR studies were performed with TaqMan Gene Expression Assays (Applied Biosystems). All experiments were conducted in triplicate. Samples were cycled 40 times with a 7300 Real Time PCR System (Applied Biosystems) as follows: 2 min at 50 °C and 10 min at 95 °C, followed by 40 cycles of 15 s at 95 °C and 1 min at 60 °C. Relative changes in expression were calculated according to the $\Delta\Delta C_T$ method using *GAPDH* as the endogenous control.

2.11. Enzyme-linked immunosorbent assay (ELISA)

NCFs and ADFs were seeded onto 10 cm dishes. After incubation for 3 days in DMEM supplemented with 10% FBS, cells were washed with PBS thoroughly 3 times and medium was changed to serum-free DMEM. After incubation for 24 h in serum-free medium, supernatant was collected as CM and contaminated cells were removed using a 0.45-μm filter (BD Falcon). VCAM-1 release in culture supernatant was measured by ELISA (R&D systems), according to the manufacture's instruction.

2.12. Neutralizing antibody assays

After pretreatment with 10 μg/mL neutralizing antibodies for 30 min, fibroblasts were seeded onto the upper surface of two-chamber culture dishes at 2.4×10^5 cells/dish, while mouse ESC-derived cardiomyocytes were seeded onto the lower surface at 4.8×10^5 cells/dish. The culture medium containing the antibody (10 μg/mL) was changed every day for 5 days. The following antibodies and culture dishes were used for neutralizing antibody assays: anti-VCAM-1 (LifeSpan Biosciences, Seattle, WA); anti-integrin α4β1 (Santa Cruz), and goat IgG isotype control (LifeSpan Biosciences). Cell culture inserts for 24-well plates (0.4 μm pores, translucent, High Density PET Membrane) were from BD Pharmingen.

2.13. Statistical analysis

All data are presented as the mean ± SD. A significant difference among multiple means was determined by one-way ANOVA. Tukey–Kramer Multiple Comparison Tests were used for post hoc pair-wise comparisons. All statistical calculations were performed using Statcel Software. A p value of <0.05 was considered significantly different.

3. Results

3.1. Cell sheet formation using mESC-derived cardiomyocytes and fibroblasts

The vast majority of cells isolated from neonatal heart, adult heart, and adult dermal tissue had a fibroblast-like morphology (Fig. 1). Since there are no specific antibodies for fibroblasts, we examined the expression of several proteins known to be expressed by fibroblasts: DDR2 (CD167b) [10], vimentin [11], and αSMA [12]. Almost all cells co-expressed DDR2, vimentin, and αSMA, but not calponin (a smooth muscle cell marker), cytokeratin 11 (an epithelial cell marker), or neural/glial antigen 2 (NG2,

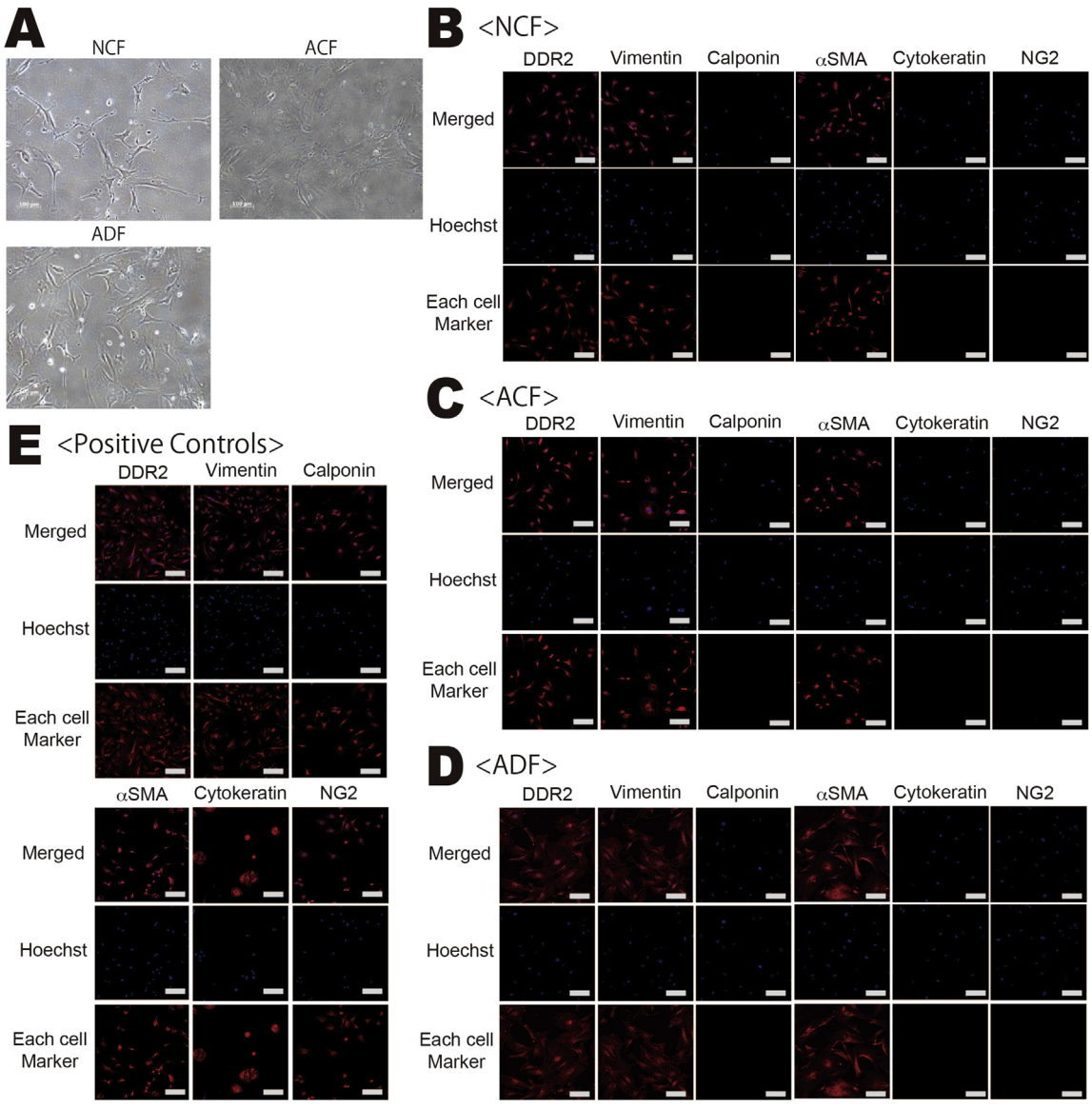

Fig. 1. Microscopic characterization of NCFs, ACFs, and ADFs. (A) Bright field microscopic images of each fibroblast type (Scale bar = 200 μm). (B–E) Representative images of DDR2, vimentin, and αSMA immunofluorescence. Almost all fibroblasts were DDR2(+), vimentin(+), and αSMA(+) but negative for calponin, cytokeratin11, and NG2. Scale bar = 500 μm.

a pericyte marker). From these findings, we concluded that the vast majority of isolated cells were fibroblasts (ACFs, NCFs, or ADFs).

Co-culture of ESC-derived cardiomyocytes with ACFs, NCFs, or ADFs at 20 °C for five days resulted in the formation of monolayer cell sheets, while no sheets were formed in the absence of fibroblasts (Fig. 2A). When cardiomyocytes were co-cultured with ACFs or NCFs, beating cardiomyocytes were numerous and equally distributed over the sheet area (Video 1, Video 2). In contrast, when cardiomyocytes were co-cultured with ADFs, beating cells were sparse and aggregated into smaller punctate regions Video 3.

Supplementary data related to this article can be found online at http://dx.doi.org/10.1016/j.reth.2016.01.005.

Electrophysiological measurements using a MED system [8,13] confirmed the microscopic determination of functional (beating) cardiomyocyte number and distribution (Fig. 2B). Extracellular action potentials (APs) were observed from many more electrode sites in cell sheets derived using ACFs or NCFs co-culture compared to cell sheets derived using ADFs co-culture.

To confirm these differences in cardiomyocyte distribution among cell sheets, co-cultures of fibroblasts and ESC-derived myocytes expressing YFP were immunostained and imaged using confocal microscopy. The number of YFP(+)/cTnT(+) cells was significantly higher in cell sheets with ACFs or NCFs than in cell sheets with ADFs (Fig. 2C–D). In fact, the number of cardiomyocytes in cell sheets with ADFs was comparable to that in cultures without fibroblasts (monocultures). There was no significant difference in cardiomyocyte number between ACFs-derived and NCFs-derived cell sheets.

3.2. Cardiomyocyte proliferation in cell sheets

To examine the mechanisms for enhanced cardiomyocyte number in the presence of cardiac fibroblasts (ACFs and NCFs compared to ADFs and fibroblast-free cultures), cultures were examined on Day 1 and Day 5 after seeding (Fig. 3A–B). On Day 1, the number of cardiomyocytes was identical among co-culture conditions, suggesting that fibroblast type did not affect the

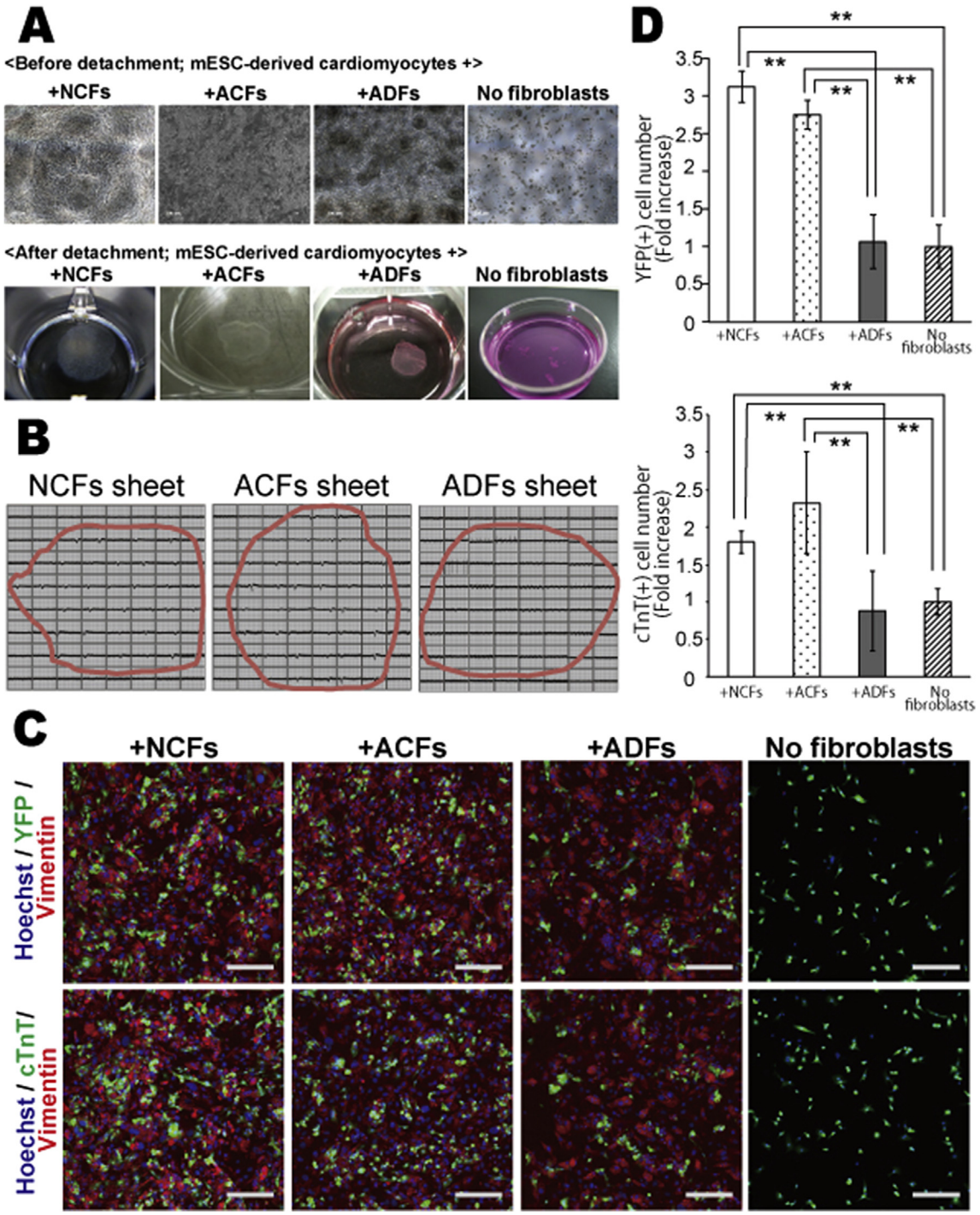

Fig. 2. Differences in cardiomyocyte number and distribution in cell sheets co-cultured with mouse neonatal cardiac fibroblasts (NCFs), adult cardiac fibroblasts (ACFs), or adult dermal fibroblasts (ADFs). Mouse embryonic stem cell (ESC)-derived cardiomyocytes were cultured with NCFs, ACFs, or ADFs, or cultured alone (monoculture). (A) Evaluation of cardiac cell sheet formation with and without each fibroblast type. (B) Extracellular action potentials recorded in cell sheets derived from NCFs, ACFs, and ADFs co-cultures and from cardiomyocyte monocultures. (Red circles show the edges of the cell sheet). (C) Immunocytochemical analysis of each co-culture system using confocal microscopy; YFP/cTnT (green), vimentin (red), Hoechst 33258 (blue nuclei), scale bar = 500 μm. (E) Bar graph representing the fold increase in YFP(+)/cTnT(+) cell number in each cell culture condition. The YFP(+)/cTnT(+) cell number in fibroblast-free cultures (fibroblast(−)) was set at 1.0 (N = 3, **P < 0.01).

initial adherence of cardiomyocytes after seeding. In co-culture with ACFs or NCFs, the number of YFP(+)/cTnT(+) cardiomyocytes on Day 5 was significantly higher than on Day 1, while there was no significant increase in cardiomyocytes in co-cultures with ADFs or in myocyte monocultures. Time-lapse image analysis of co-cultures containing YFP(+) cardiomyocytes and fibroblasts isolated from DsRed mice (expressing red fluorescent protein under control of the CAG promoter) showed that cardiomyocytes migrated, proliferated, and formed an interacting network with NCFs (Video 4). Conversely, cardiomyocytes showed less proliferation in co-culture with ADFs and did not construct such a network (Video 5).

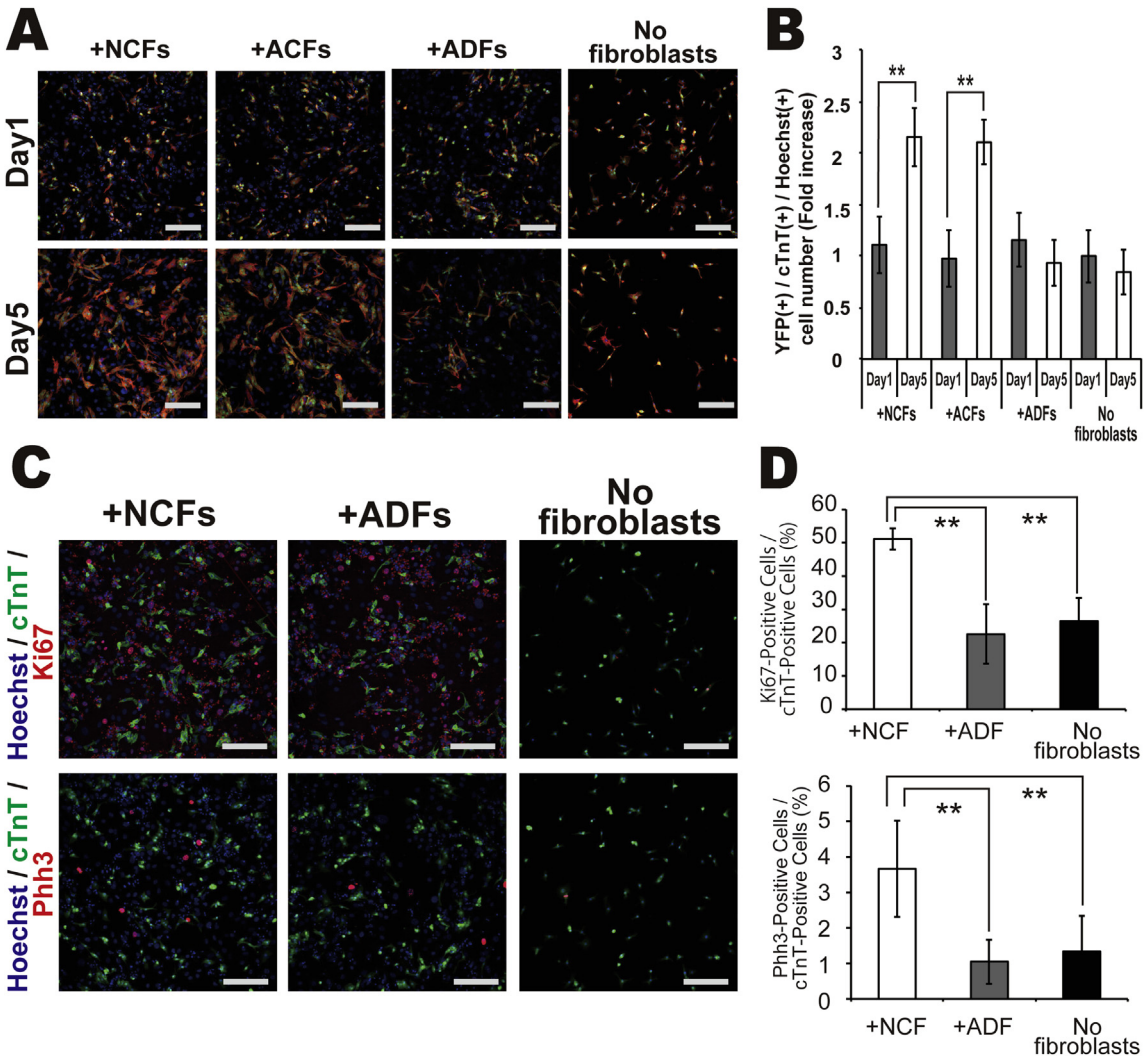

Fig. 3. Changes in cardiomyocyte number from Day 1 to Day 5 in each culture condition. (A) Immocytochemical analysis of cell numbers under each cell condition on Day 1 and Day 5; YFP (green), cTnT (red), Hoechst 33258 (blue nuclei), scale bar = 500 μm. (B) Number of cardiomyocytes/culture. Bar graphs depict the fold increase in YFP(+)/cTnT(+) cells. The value for fibroblasts(−) cultures on Day1 is set at 1.0 (N = 3, **P < 0.01). (C–D) Staining for cell proliferation markers Ki67 and Phh3 cardiomyocytes under each culture condition; cTnT (green), Ki67/Phh3 (red), and Hoechst 33258 (blue nuclei), scale bar = 500 μm (N = 4, **P < 0.01).

Supplementary data related to this article can be found online at http://dx.doi.org/10.1016/j.reth.2016.01.005.

The differential proliferation of cardiomyocytes among co-culture conditions was confirmed by immunocytochemical analysis. The percentage of YFP(+) cardiomyocytes expressing the mitotic markers Ki67 and phospho-histone H3 (Phh3) was significantly higher in co-cultures with NCFs than in co-cultures with ADFs or in myocyte monocultures (Fig. 3C–D). BrdU incorporation by cardiomyocytes was significantly higher in co-culture with NCFs compared to co-culture with ADFs or in myocyte monocultures (Fig. 4A–B).

To investigate the underlying mechanisms for enhanced cardiomyocyte proliferation in the presence of NCFs, mESC-derived cardiomyocytes and NCFs were cultured in separate chambers, with NCFs on the upper layer and cardiomyocytes on the lower layer, to distinguish the contribution of cell–cell contact from extracellular signaling by soluble factors (Fig. 4C). The number of cardiomyocytes on Day 5 was still markedly higher than that on Day 1 (Fig 4D), although the magnitude of the increase (~1.5 folds) was lower than that in co-culture with direct cell–cell contact (~2.5 times) (Fig. 4E). These findings suggest that both soluble factors secreted from NCFs and direct cell–cell interactions between cardiomyocytes and cardiac fibroblasts promote cardiomyocyte proliferation.

3.3. *Identification of fibroblast–cardiomyocyte signaling factors by comparative analysis of fibroblasts gene expression*

To identify the factors responsible for enhanced cardiomyocyte proliferation secreted by NCFs, we performed a comprehensive analysis of gene expression differences between each type of fibroblast (NCFs and ADFs) using microarrays. Many genes were differentially expressed between NCFs and ADFs (Fig. 5A), with over 500 genes showing greater than 10-fold enhancement of expression in NCFs compared to ADFs (Supplementary Table 1). Of these, 21 genes were cardiovascular-related (Table 1). When we selected genes that are either embryonic lethal when knocked out and/or encode soluble factors, only VCAM-1 remained. The greater expression of VCAM-1 in NCFs compared to ADFs was confirmed by quantitative RT-PCR and ELISA (Fig. 5B–C).

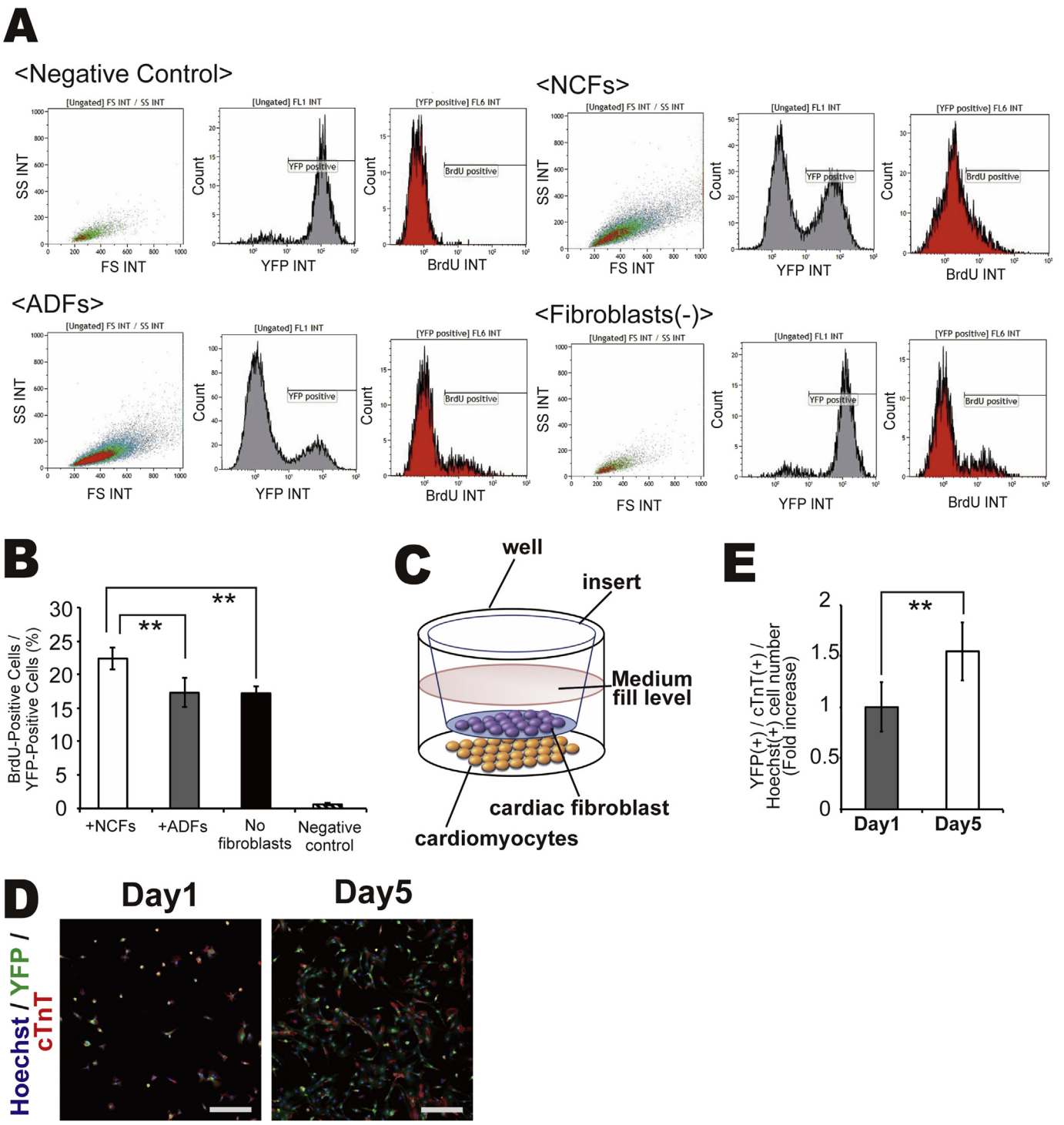

Fig. 4. (A–B) BrdU incorporation into cardiomyocytes under each culture condition as measured by FACS (N = 3, **P < 0.01). (C–E) Immocytochemical identification of cardiomyocytes in two-chamber culture dishes on Day 1 and Day 5 by confocal microscopy; YFP (green), cTnT (red), Hoechst 33258 (blue nuclei), scale bar = 500 μm. YFP(+)/cTnT(+) cell number at Day 1 was set to 1.0 (N = 4, **P < 0.01, *P < 0.05).

3.4. VCAM-1-dependent cardiomyocyte proliferation in co-cultures with cardiac fibroblasts

Integrin α4β1 is the principal VCAM-1 co-receptor, so we examined integrin α4β1 expression by mESC-derived cardiomyocytes. Indeed, almost all showed integrin α4β1 expression (Fig. 5D), suggesting possible responsively to fibroblast-derived VCAM-1. Next, to test whether VCAM-1 contributes to cardiac fibroblast-mediated cardiomyocyte proliferation, we examined the effects of neutralizing antibodies. After pretreatment with neutralizing antibodies on NCFs for 30 min, fibroblasts were seeded onto the upper surface of two-chamber culture dishes, while mouse ESC-derived cardiomyocytes were seeded onto the lower surface. Two-chamber co-culture of mESC-derived cardiomyocytes

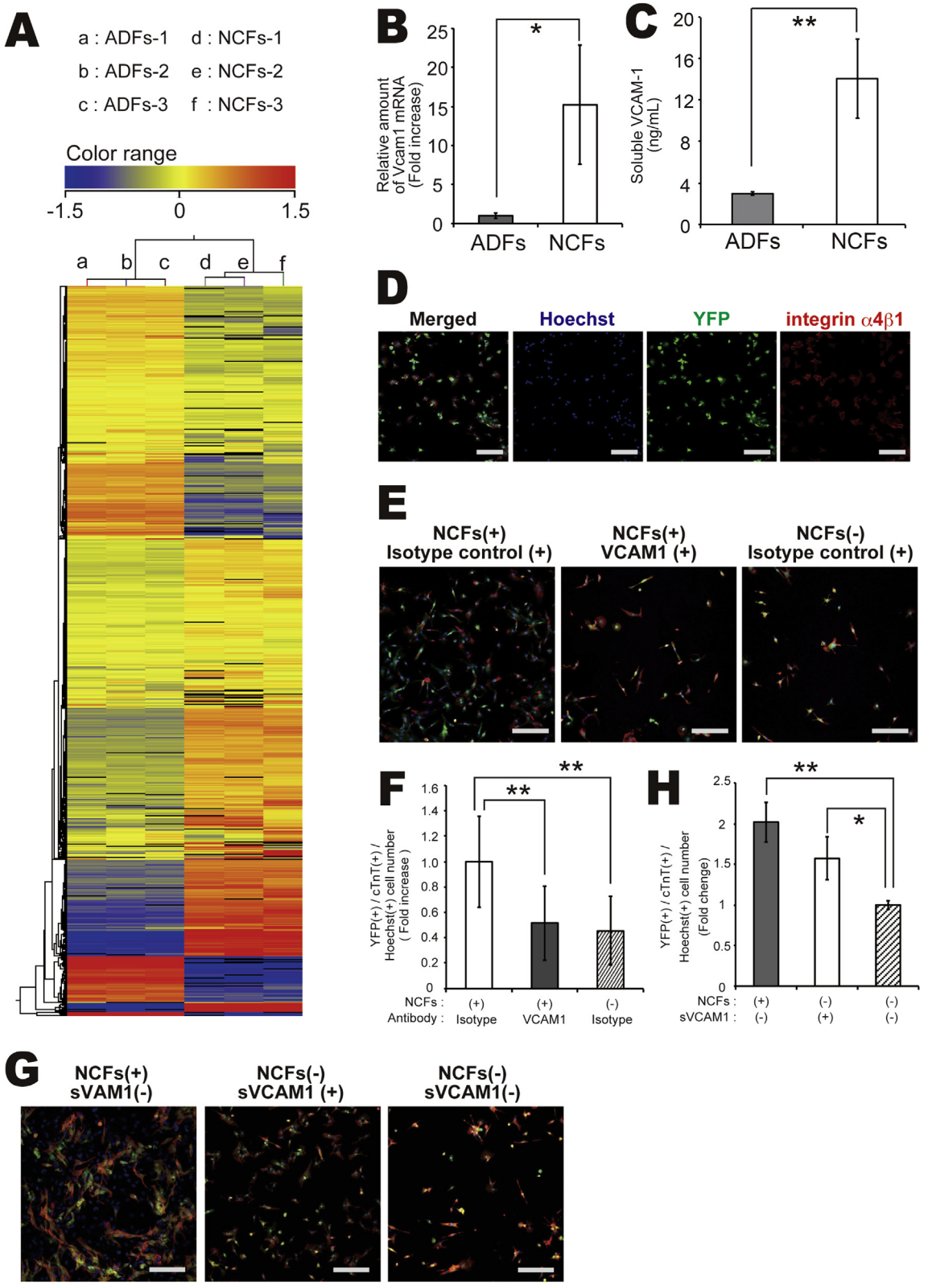

Fig. 5. (A) Comprehensive genetic cluster analysis of ADFs and NCFs. (B) Expression levels of the VCAM-1 gene in NCFs and ADFs as measured by real-time PCR (N = 3, *P < 0.05). (C) VCAM-1 protein expression levels in conditioned medium of NCFs and ADFs as measured by enzyme-linked Immunosorbent assay (ELISA) (N = 4, **P < 0.01). (D) Immunocytochemical imaging of VCAM-1 co-receptor integrin α4β1 surface expression by mESC-derived cardiomyocytes; cTnT (green), integrin α4β1 (red), and Hoechst 33258 (blue nuclei), Scale bar = 500 μm. (E–F) Effect of neutralizing antibodies on cardiomyocyte number on Day 5 in two-chamber culture; YFP (green), cTnT (red), and Hoechst 33258 (blue nuclei). Scale bar = 500 μm, N = 3, **P < 0.01. (G–H) Effect of VCAM-1 (soluble protein) on cardiomyocyte number on Day 5; YFP (green), cTnT (red), and Hoechst33258 (blue nuclei). Scale bar = 500 μm (N = 3, *P < 0.05, **P < 0.01).

Table 1
Cardiovascular system-related genes showing greater than 10-fold higher expression in NCFs compared with ADFs (N = 3).

Gene name	FCAbsolute
Chemokine (C-X-C motif) ligand 12 (Cxcl12)	89.99
Forkhead box S1 (Foxs1)	72.43
Troponin T2, cardiac (Tnnt2)	65.35
Zinc finger protein, multitype 2 (Zfpm2)	49.07
Protein tyrosine phosphatase, receptor type, B (Ptprb)	44.6
Insulin-like growth factor 1 (Igf1)	36.36
Wilms tumor 1 homolog (Wt1)	31.28
Thromboxane A2 receptor (Tbxa2r)	28.95
Collagen, type VIII, alpha 1 (Col8a1)	26.44
A disintegrin-like and metallopeptidase (reprolysin type) with thrombospondin type 1 motif, 1 (Adamts1)	23.86
Lysyl oxidase (Lox)	23.73
c-fos induced growth factor (Figf)	23.16
Vascular cell adhesion molecule 1 (Vcam1)	21.77
Forkhead box C2 (Foxc2)	21.45
Collagen, type XI, alpha 1 (Col11a1)	20.76
Odd-skipped related 1 (Drosophila) (Osr1)	18.28
Fibroblast growth factor 18 (Fgf18)	16.95
Neuropilin 1 (Nrp1)	14.16
Meis homeobox 1 (Meis1)	12.45
Plasminogen activator, urokinase (Plau)	11.28

FCAbsolute: Absolute fold change in gene expression.

with NCFs pretreated with anti-VCAM-1 and in the continued presence of medium plus anti-VCAM-1 resulted in a substantial inhibition of cardiomyocyte proliferation compared to two-chamber co-culture with untreated NCFs in regular medium (Fig. 5E–F).

Finally, we evaluated the direct (cell contact-dependent) effects of VCAM-1 on the proliferation of cardiomyocytes. One day after seeding, cardiomyocyte monocultures were treated with VCAM-1 until Day 5. Like the presence of NCFs, VCAM-1 treatment increased the number of cardiomyocytes compared to untreated monocultures (Fig. 5G–H). Moreover, the number of cardiomyocytes on Day 5 was comparable to that in co-cultures with NCFs. These findings suggest that cardiac fibroblasts induce cardiomyocyte proliferation through expression and release of VCAM-1.

4. Discussion

Fibroblasts participate in heart development and in the pathogenesis of cardiovascular diseases. The presence of fibroblasts is also critical for the efficient fabrication of bioengineered cardiac tissue sheets for transplantation and *in vitro* studies. These effects, which enhance cardiomyocyte proliferation and create cardiac sheets observed in extracellular APs from all electrode sites, involve cell–cell interactions between fibroblasts and surrounding cardiomyocytes, but the signaling mechanisms remain obscure. In this study, we demonstrate for the first time the importance of fibroblast source for fabricating functional bioengineered cardiac tissue using ESC-derived cardiomyocytes. Fibroblasts from heart tissue were superior to fibroblasts from dermal tissue for fabrication of cardiac cell sheets as NCFs-derived sheets exhibited many more functional (beating) cardiomyocytes. This increase in functional cardiomyocytes was due to the greater NCFs expression of VCAM-1, which alone enhanced the cardiomyocyte proliferation.

Bioengineered cardiac tissue sheets can be used for cell-based therapy or to establish more realistic *in vitro* tissue models. In general, pluripotent stem cell-derived cardiomyocytes are used because bioengineered cardiac tissue requires a high-yielding source of myocyte precursors. As cardiomyocytes are responsible for generating the contractile force of cardiac tissue, the number of cardiomyocytes in cell sheets is thought to correlate with the functional utility for clinical applications. In addition, efficient force generation requires the optimal spatial distribution of contractile cells. Both of these criteria were fulfilled by co-culturing ESC-derived cardiomyocytes with cardiac fibroblasts; whereas, dermal fibroblast co-culture resulted in fewer cells that were aggregated in punctuate regions of the sheet. In this study, we found that the optimum mESC-derived cardiomyocytes to cardiac fibroblast ratio was 8:2 as previously reported [8]; therefore, efficient generation of cell sheets does not require high seeding density when using NCFs. Furthermore cardiac fibroblasts have been reported to promote the differentiation of mouse ES cells into mature cardiomyocytes in three-dimensional indirect co-culture condition [14]. Collectively the presence of cardiac fibroblasts might be quite important to fabricate functional cardiac tissues via increasing number of cardiomyocytes and promoting cardiomyocyte maturation.

Several recent studies have reported the proliferative effects of growth factors, including granulocyte colony stimulating factor [15], and signaling agents such as p38MAPK inhibitors [16], on cardiomyocytes. However, few reports have identified the signaling mechanisms mediating the interactions between cardiomyocytes and cardiac fibroblasts; mechanisms that may be exploited for enhanced cardiomyocyte proliferation to produce superior bioengineered cardiac tissue. Several groups, including ours, have reported that co-culture with cardiac fibroblasts is indispensable for fabricating cardiac tissue, possibly due to the insufficient secretion of extracellular matrix by cardiomyocytes alone [8,17]. In this study, cardiac cell sheets obtained using cardiac fibroblasts in co-culture resulted in more numerous functional cardiomyocytes, suggesting that endogenous fibroblasts possess unique properties conducive to cardiomyocyte proliferation and function. Indeed, fibroblasts from heart expressed substantially higher levels of VCAM-1 than dermal fibroblasts, resulting in faster myocyte proliferation. VCAM-1 was reported to be also expressed on human ES/iPS cell-derived cardiomyocytes [18]. In the present study, the increase of cell number of mouse ES cell derived cardiomyocytes was not observed without the existence of NCFs (Fig. 2 C–D, Figs. 3 and 4 A–B). Although we did not examine the expression levels of VCAM-1 on mouse ES-derived cardiomyocytes, NCFs might express more abundant VCAM-1 than cardiomyocytes enough to induce the proliferation of cardiomyocytes.

Cardiac fibroblasts originate from multiple sources during heart development [12]. Those normally present in the cardiac interstitium and annulus fibrosus are derived from the embryonic proepicardium. Embryonic proepicardium-derived cells migrate to the surface of the fetal heart and form an epicardium. Cells in the epicardium then differentiate into cardiac fibroblasts through epithelial–mesenchymal transition (EMT) triggered by platelet-derived growth factor (PDGF), fibroblast growth factor (FGF), and transforming growth factor β (TGF-β) [19,20]. On the other hand, the endothelial cells located in the atrioventicular cushion migrate into the cardiac jelly and acquire the cardiac fibroblast phenotype through endothelial–mesenchymal transition (EndMT) triggered by TGF-β, PDGF, and Wnt [21]. In this study, we found that cardiac fibroblasts abundantly expressed VCAM-1, a ligand for α4β1 integrin expressed by cardiomyocytes. We previously reported that soluble VCAM-1 secreted from cardiac progenitor cells showed the cardioprotective effects through α4β1 integrin-mediated activation of Akt, ERK and P38MAPK in cardiomyocytes. This interaction has been reported to be also critical for heart development [22,23]. Kwee et al. [20] reported that VCAM-1 was expressed at the outer myocardial layer, but not at the endocardial cushion at E11.5, while α4 integrin was expressed by a single layer of epicardial cells. Furthermore, VCAM-1-deficient embryos exhibited reduced thickness of the ventricular myocardium concomitant with the loss of

epicardial cells at E11.5 [22]. Yang et al. [21] reported the loss of epicardium in α4 integrin-null embryos at E11.5 [23]. Therefore, the VCAM-1/α4 integrin interaction may be the predominant signal for formation of epicardium at the embryonic stage. In light of the dramatic proliferative effect of cardiac fibroblasts on mouse ESC-derived cardiomyocytes through VCAM-1, we suggest that the cardiac fibroblasts used in this study may have originated primarily from epicardium.

VCAM-1 is known to exist as both a transmembrane protein and in a soluble form. When mESC-derived cardiomyocytes were co-cultured with cardiac fibroblasts, the number of cardiomyocytes was increased up to 2.5 folds in 5 days (Fig. 2A–B), while the increase was only about 1.5 folds when cells were co-cultured in two-chamber culture plates allowing macromolecule diffusion but no direct cell–cell contact (Fig. 2F–G). Therefore, cardiac fibroblasts appear to induce cardiomyocyte proliferation via both direct VCAM-1-mediated cell–cell contact and by extracellular signaling via soluble VCAM-1. Moreover, cardiomyocyte α4β1 integrin appears critical for cell adhesion, as in leukocytes and endothelial cells [24].

The number of cardiomyocytes 1 day after culture seeding was identical among co-cultures containing different fibroblast types. However, the number of cardiomyocytes increased substantially after 5 days when co-cultured with cardiac fibroblasts despite a substantial loss of nonadherent (floating) cells on Day 1 in all cultures, suggesting that the increased cardiomyocyte number in co-culture with cardiac fibroblasts was not due to an early increase in cell adhesion.

Some extracellular matrix proteins have been reported to regulate the proliferation of cardiomyocytes under special conditions. Periostin is expressed in the developing and post-infarct heart, but not in the mature healthy heart [25]. Administration of periostin in the postnatal period induced cell cycle reentry of differentiated cardiomyocytes through integrin αv-, β1-, β3-, and β5-mediated activation of the PI3 kinase and Akt pathways [26]. We previously reported that VCAM-1 activated Akt, Erk, and p38MAPK in neonatal rat cardiomyocytes through α4β1 integrin and prevented cardiomyocyte damage from oxidative stress [26,27]. Since almost all ESC-derived cardiomyocytes expressed α4β1 integrin under our culture conditions, activation of Akt may be important for VCAM-1-mediated proliferation of ESC-derived cardiomyocytes.

There are a few limitations to this study. We used cells isolated from neonatal and adult mouse hearts as cardiac fibroblasts, and cells isolated from adult mouse dermal tissue as dermal fibroblasts. Although almost all of these cells resembled fibroblasts morphologically and were positive for DDR2, vimentin, and αSMA, we cannot exclude the possibility that these populations also contained other cell types. Moreover, over 500 genes were differentially expressed between cardiac- and dermal-derived fibroblasts; therefore, we cannot eliminate the contribution of other factors to cardiomyocyte proliferation. However, only VCAM-1 has been linked to cardiovascular development and function, and a VCAM-1 antibody completely abolished the proliferative effect.

In sum, these results demonstrate that co-culture with cardiac fibroblasts improves the fabrication of functional bioengineered cardiac tissue through VCAM-1-mediated stimulation of cardiomyocyte proliferation. Understanding the molecular mechanisms mediating cell–cell signaling between cardiomyocytes and cardiac fibroblasts may provide new insights in cardiac development and pathogenesis, and lead to improved methods for fabrication of bioengineered heart tissue. Our next challenge is to demonstrate these effects in human cells and identify the molecular signaling mechanisms that trigger cardiomyocyte proliferation after VCAM-1 stimulation by cardiac fibroblasts.

Acknowledgments

We thank Y. Haraguchi, D. Sasaki, and N. Yasuda for their excellent technical advice and K. Sugiyama, M. Anazawa, T. Ikeda, and F. Kodama for technical assistance. This study was supported by grants from the Japan Society for the Promotion of Science through the “Funding Program for World-Leading Innovative R&D on Science and Technology (FIRST Program)” initiated by the Council for Science and Technology Policy (CSTP), and an open research grant from The Japan Research Promotion Society for Cardiovascular Disease and JSPS KAKENHI (Grant number 25-57082).

Appendix A. Supplementary data

Supplementary data related to this article can be found at http://dx.doi.org/10.1016/j.reth.2016.01.005.

References

[1] Souders CA, Bowers SLK, Baudino TA. Cardiac fibroblast: the renaissance cell. Circ Res 2009;105:1164–76. http://dx.doi.org/10.1161/CIRCRESAHA.109.209809.
[2] Brown RD, Ambler SK, Mitchell MD, Long CS. The cardiac fibroblast: therapeutic target in myocardial remodeling and failure. Annu Rev Pharmacol Toxicol 2005;45:657–87. http://dx.doi.org/10.1146/annurev.pharmtox.45.120403.095802.
[3] Fujisaki H, Ito H, Hirata Y, Tanaka M, Hata M, Lin M, et al. Natriuretic peptides inhibit angiotensin II-induced proliferation of rat cardiac fibroblasts by blocking endothelin-1 gene expression. J Clin Invest 1995;96:1059–65. http://dx.doi.org/10.1172/JCI118092.
[4] Ieda M, Tsuchihashi T, Ivey KN, Ross RS, Hong T, Shaw RM, et al. Cardiac fibroblasts regulate myocardial proliferation through B1 integrin signaling. Dev Cell 2009;16:233–44. http://dx.doi.org/10.1016/j.devcel.2008.12.007.Cardiac.
[5] Shimizu T, Yamato M, Isoi Y, Akutsu T, Setomaru T, Abe K, et al. Fabrication of pulsatile cardiac tissue grafts using a novel 3-dimensional cell sheet manipulation technique and temperature-responsive cell culture surfaces. Circ Res 2002;90:e40. http://dx.doi.org/10.1161/hh0302.105722.
[6] Sekiya S, Shimizu T, Yamato M, Kikuchi A, Okano T. Bioengineered cardiac cell sheet grafts have intrinsic angiogenic potential. Biochem Biophys Res Commun 2006;341:573–82. http://dx.doi.org/10.1016/j.bbrc.2005.12.217.
[7] Shimizu T, Yamato M, Kikuchi A, Okano T. Cell sheet engineering for myocardial tissue reconstruction. Biomaterials 2003;24:2309–16. http://dx.doi.org/10.1016/S0142-9612(03)00110-8.
[8] Matsuura K, Masuda S, Haraguchi Y, Yasuda N, Shimizu T, Hagiwara N, et al. Creation of mouse embryonic stem cell-derived cardiac cell sheets. Biomaterials 2011;32:7355–62. http://dx.doi.org/10.1016/j.biomaterials.2011.05.042.
[9] Deschamps AM, Spinale FG. Disruptions and detours in the myocardial matrix highway and heart failure. Curr Heart Fail Rep 2005;2:10–7. http://dx.doi.org/10.1007/s11897-005-0002-6.
[10] Makino K, Jinnin M, Aoi J, Hirano A, Kajihara I, Makino T, et al. Discoidin domain receptor 2–microRNA 196a–mediated negative feedback against excess type I collagen expression is impaired in scleroderma dermal fibroblasts. J Invest Dermatol 2012;133. http://dx.doi.org/10.1038/jid.2012.252.
[11] Franke WW, Weber K, Osborn M, Schmid E, Freudenstein C. Antibody to prekeratin. Decoration of tonofilament like arrays in various cells of epithelial character. Exp Cell Res 1978;116:429–45.
[12] Snider P, Standley KN, Wang J, Azhar M, Doetschman T, Conway SJ. Origin of cardiac fibroblasts and the role of periostin. Circ Res 2009;105:934–47. http://dx.doi.org/10.1161/CIRCRESAHA.109.201400.
[13] Haraguchi Y, Shimizu T, Yamato M, Kikuchi A, Okano T. Electrical coupling of cardiomyocyte sheets occurs rapidly via functional gap junction formation. Biomaterials 2006;27:4765–74. http://dx.doi.org/10.1016/j.biomaterials.2006.04.034.
[14] Ou D-B, He Y, Chen R, Teng J-W, Wang H-T, Zeng D, et al. Three-dimensional co-culture facilitates the differentiation of embryonic stem cells into mature cardiomyocytes. J Cell Biochem 2011;112:3555–62. http://dx.doi.org/10.1002/jcb.23283.
[15] Shimoji K, Yuasa S, Onizuka T, Hattori F, Tanaka T, Hara M, et al. G-CSF promotes the proliferation of developing cardiomyocytes in vivo and in derivation from ESCs and iPSCs. Cell Stem Cell 2010;6:227–37. http://dx.doi.org/10.1016/j.stem.2010.01.002.
[16] Engel FB, Hsieh PCH, Lee RT, Keating MT. FGF1/p38 MAP kinase inhibitor therapy induces cardiomyocyte mitosis, reduces scarring, and rescues function after myocardial infarction. Proc Natl Acad Sci U S A 2006;103:15546–51. http://dx.doi.org/10.1073/pnas.0607382103.
[17] Liau B, Christoforou N, Leong KW, Bursac N. Pluripotent stem cell-derived cardiac tissue patch with advanced structure and function. Biomaterials 2011;32:9180–7. http://dx.doi.org/10.1016/j.biomaterials.2011.08.050.

[18] Uosaki H, Fukushima H, Takeuchi A, Matsuoka S, Nakatsuji N, Yamanaka S, et al. Efficient and scalable purification of cardiomyocytes from human embryonic and induced pluripotent stem cells by VCAM1 surface expression. PLoS One 2011;6:e23657. http://dx.doi.org/10.1371/journal.pone.0023657.
[19] Lu J, Landerholm TE, Wei JS, Dong XR, Wu SP, Liu X, et al. Coronary smooth muscle differentiation from proepicardial cells requires rhoA-mediated actin reorganization and p160 rho-kinase activity. Dev Biol 2001;240:404–18. http://dx.doi.org/10.1006/dbio.2001.0403.
[20] Morabito CJ, Kattan J, Bristow J. Mechanisms of embryonic coronary artery development. Curr Opin Cardiol 2002;17:235–41. http://dx.doi.org/10.1097/00001573-200205000-00005.
[21] Zavadil J, Böttinger EP. TGF-beta and epithelial-to-mesenchymal transitions. Oncogene 2005;24:5764–74. http://dx.doi.org/10.1038/sj.onc.1208927.
[22] Kwee L, Baldwin HS, Shen HM, Stewart CL, Buck C, Buck C a, et al. Defective development of the embryonic and extraembryonic circulatory systems in vascular cell adhesion molecule (VCAM-1) deficient mice. Development 1995;121:489–503.
[23] Yang JT, Rayburn H, Hynes RO. Cell adhesion events mediated by alpha 4 integrins are essential in placental and cardiac development. Development 1995;121:549–60.
[24] Muller WA. Mechanisms of transendothelial migration of leukocytes. Circ Res 2009;105:223–30. http://dx.doi.org/10.1161/CIRCRESAHA.109.200717.
[25] Morin N a, Oakes PW, Hyun Y-M, Lee D, Chin YE, King MR, et al. Nonmuscle myosin heavy chain IIA mediates integrin LFA-1 de-adhesion during T lymphocyte migration. J Exp Med 2008;205:195–205. http://dx.doi.org/10.1084/jem.20071543.
[26] Kühn B, del Monte F, Hajjar RJ, Chang Y-S, Lebeche D, Arab S, et al. Periostin induces proliferation of differentiated cardiomyocytes and promotes cardiac repair. Nat Med 2007;13:962–9. http://dx.doi.org/10.1038/nm1619.
[27] Matsuura K, Honda A, Nagai T, Fukushima N, Iwanaga K, Tokunaga M, et al. Transplantation of cardiac progenitor cells ameliorates cardiac dysfunction after myocardial infarction in mice. J Clin Invest 2009;119:2204–17. http://dx.doi.org/10.1172/JCI37456.